10IKC-195

HETEROGENEOUS MANTLE BENEATH THE LUNDA AREA IN ANGOLA: Nd ISOTOPIC EVIDENCE

Robles-Cruz*[a]SE, Galí[a]S, Escayola[b]M, and Melgarejo[a]JC

[a]*Departament de Cristal·lografia, Mineralogia i Dipòsits Minerals, Universitat de Barcelona, Barcelona, Spain ([*]sandra_robles@ub.edu)*
[b]*CONICET-IDEAN Instituto de Estudios Andinos, Universidad de Buenos Aires, Buenos Aires, Argentina*

1. Introduction

Investigations into regional setting of kimberlites, their mineralogy and geochemistry, and more specifically the study of xenoliths from kimberlites, have provided valuable information about the nature of the upper mantle beneath old continental cratons (Macdougall and Haggerty, 1999). Information about isotopic composition of these xenoliths provides a more direct means of examining the chemical evolution of the sub-continental lithosphere. Radiogenic isotopes (e.g., Sm/Nd) can be used to determine the age of xenoliths and to better understand their origen.

In this study we examine the Sm/Nd isotopes of xenoliths from three Angola kimberlites: the Catoca (CA), Cucumbi-79 (CU79), and Cucumbi-80 (CU80) pipes (Fig.1). The CA, CU79, and CU80 kimberlite pipes are located in Angola in the Lunda Sul and Lunda Norte provinces, respectively (Fig. 1). The CA kimberlite is one of the largest primary diamond deposits worldwide. The CU79 is a diamondiferous pipe but without significant diamond production, while the CU80 pipe has been reported as non productive because preliminary petrological analyses of the pipe indicated a low probability of it being diamondiferous and for that reason no additional tests were subsequently carried out. (oral communication Dr. S. Pereira, 2007).

Angola has a complex geological history in which kimberlites intrude Archean basement rocks of the Kasai-Congo Craton. The tectonic framework of Angola has played an important role not only in producing mantle upwelling and kimberlitic magmatism, but also in the evolution of the host rocks. The Lower Cretaceous regional extension determined the development of deep faults and grabens with trends NE-SW and NW-SE. The Lucapa structure corresponds to the first group, and the northeastern part of the Lucapa structure is where most of the diamondiferous kimberlites in Angola are found. In contrast the southwestern zone has a high presence of undersaturated alkaline rocks and carbonatites (Reis, 1972). Other minor kimberlite fields are found in SW Angola (Egorov et al., 2007). This geological configuration likely acted as a tectonic control on the presence and distribution of kimberlites in Angola.

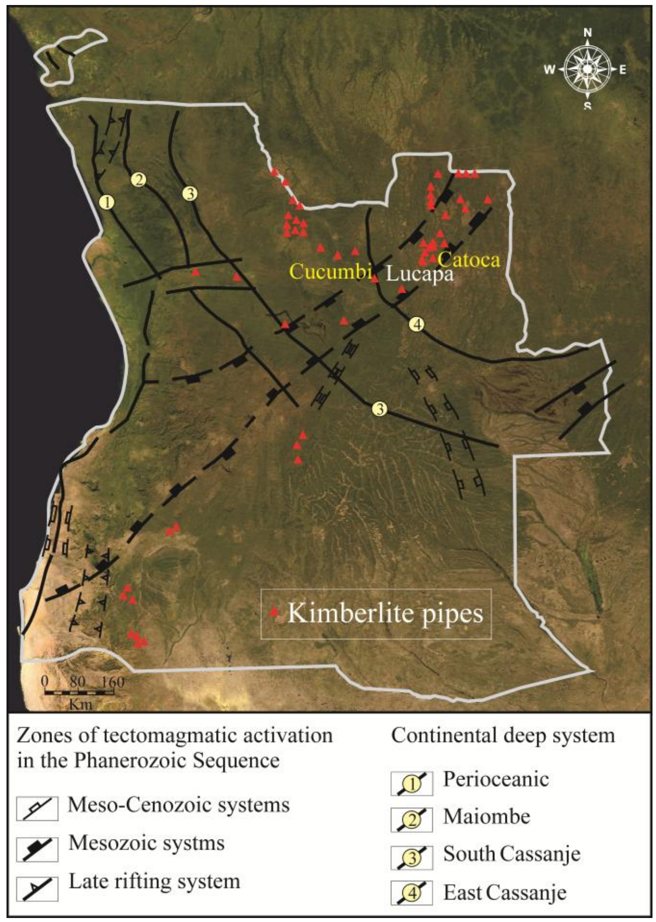

Fig. 1. Geological setting of Angola kimberlites (modified from Perevalov et al., 1992; Egorov et al., 2007).

2. Samples and analytical techniques

This study presents accurate high precision Sm/Nd isotopic compositions for ten samples of xenoliths from three Angolan kimberlites (CA, CU79, and CU80). The selected

xenoliths range from 1.5 to 7 cm. Optical petrographic studies and BSE images from SEM-ESEM with EDS microanalysis and electron probe microanalysis (EPMA) allowed the authors to discriminate the main types of xenoliths and to select ten representative samples (Table 1).
Trace element analyses of garnet, clinopyroxene, and ilmenite from xenoliths, and xenocrysts (olivine, garnet, clinopyroxene, and ilmenite) from the CA and CU79 kimberlite pipes had previously been performed by laser ablation inductively coupled plasma mass spectrometry (LA-ICP-MS) at the Geological Survey of Canada (Ottawa) (Robles-Cruz et al., 2011 in preparation) in order to complete the mineral characterization of these two diamondiferous kimberlites.

Table 1. Description of xenoliths

No.	Sample name	Xenolith type	Net sample (mg)	Minerals
1*	CA-77/35-398.2	garnet-lherzolite	466.22	pyrope-clinopyroxene
2*	CA-335-560	garnet-phlogopite-lherzolite	397.51	pyrope-clinopyroxene-ilmenite-phlogopite
3	CA-335-607C	eclogite	393.69	pyrope-omphacite
4*	CA-535-479.6-39	carbonatite	433.04	calcite-ilmenite-apatite
5*	CU79-58.7	glimmerite	417.50	phlogopite-ilmenite
6	CU79-99.5	phlogopite-rich	460.02	mica-amphibole-ilmenite-diopside
7*	CU79-130	PIC	508.09	phlogopite-ilmenite-clinopyroxene
8*	CU79-134B	garnet-lherzolite	319.09	pyrope-serpentine-clinopyroxene
9*	CU79-189	garnet-lherzolite	381.92	pyrope-serpentine-clinopyroxene-ilmenite
10*	CU80-56	phlogopite-rich	449.09	phlogopite-hematite-ilmenite-calcite

(*) Selected for Sm/Nd analyses

Eight of these xenoliths were selected to perform Sm/Nd isotopic analyses (Table 1) to get information about the mantle source and age data. The Sm/Nd isotopic analyses were carried out at the Pacific Centre for Isotopic and Geochemical Research (PCIGR) at the University of British Columbia, using a Thermo Finnigan Triton thermo-ionization mass spectrometer (TIMS). We used the analytical procedures for sample dissolution, ion exchange, and leaching described by Weis et al. (2006, and references therein). The normalization procedure has been applied to the Nd isotopic ratios using La Jolla Nd as the reference material.

3. Results and Discussion

3.1. Rare earth element (REE) composition

The trace elements analyses of xenoliths (Robles et al., 2011 in preparation) and xenocrysts from the CA and CU-79 pipes allowed the authors to identify two main types of normalized REE distribution for garnet in the CA kimberlite: eclogitic garnet which exhibits "normal" (McLean et al., 2007) REE_N patterns, and lherzolitic garnet (lherzolite with less than 5% of phlogopite) which usually has "sinusoidal" REE_N patterns and rarely "normal" REE_N patterns. Unlike in CU79, garnet from lherzolite xenoliths presents "normal" patterns with lower REE values, only clinopyroxene from phlogopite-rich xenoliths exhibits higher values in LREE than the same xenoliths in the CA kimberlite. These two kimberlites have sampled sources under different equilibration conditions and degrees of metasomatism. Hence, the "sinusoidal" pattern exhibited by lherzolitic garnet from the CA kimberlite might be the result of refertilization of previously depleted peridotite by different degrees of re-enrichment in incompatible elements. The "normal" patterns in the CU79 pipe might reflect a depleted mantle source.

3.2.Nd isotopic compositions

Nd isotopic results are reported in Table 2a and b. This new Sm-Nd isotopes analyses, carried out on mantle xenoliths from the CA kimberlite have a $^{143}Nd/^{144}Nd$ value between 0.511288 and 0.511681, while Sm-Nd isotopes in xenoliths from the CU79 kimberlite show higher $^{143}Nd/^{144}Nd$ values between 0.512274 and 0.512391 (a narrower range of values). Only one value from the CU80 pipe was obtained 0.512377 and can be used as a comparison with the other kimberlites. Negative ε_{Nd} values from xenoliths of the CA kimberlite indicate an enriched mantle, while mantle-derived xenoliths from the CU79 pipe show a slight depleted mantle signature with positive ε_{Nd} values as well as the sample from the CU80 pipe (Table 2b, Fig. 2).

Based on the REE and Sm/Nd isotope analyses we propose a different source for both kimberlites, the CA and CU79 pipes. These two kimberlites have heterogeneous mantle sources, where the CA kimberlite is the more enriched of the two possibly due to multiple metasomatic events that could explain the "sinusoidal" REE_N patterns in garnet. Both kimberlitic mantle xenoliths also have different T_{DM} (Model ages relative to CHRUR): the CA kimberlite xenoliths show Mesoproterozoic ages (1220 - 1250 Ma), while the CU79 kimberlite xenoliths yield 450 to 390 Ma (Late Ordovician to Devonian) like the T_{DM} from CU80. These ages can be interpreted as the age of mantle generation or the age of a metasomatic event that modified the isotopic ratios in the mantle. T_{DM} model ages of 1.2 Ga or the xenoliths from the CA kimberlite are likely associated with the Kibaran orogeny, and the ages from the CU79 imply more juvenile Paleozoic components which may have been related to the assembly of Pangea. Based on this data it is clear that these two kimberlites with different diamond production grades have a different evolution despite being from the same geographical area.

Table 2a. Results of Nd Isotopic Analyses (TIMS)

No.	Age (Ma)	Sm (ppm)	Nd (ppm)	Sm/Nd	$^{147}Sm/^{144}Nd$ actual	$^{143}Nd/^{144}Nd$ actual
1	1250	2.06	8.18	0.251834	0.151600	0.512532
2	1250	2.66	15.50	0.171613	0.103300	0.512529
4	1250	19.90	227.00	0.087665	0.052800	0.511756
5	650	1.04	6.80	0.152047	0.091500	0.512781
7	650	1.19	7.80	0.152174	0.091600	0.512744
8	650	1.86	9.60	0.193750	0.116600	0.512771
9	650	0.85	5.30	0.160377	0.096500	0.512725
10	650	6.10	42.30	0.144208	0.086800	0.512747

Table 2b. Results of Nd Isotopic Analyses (TIMS)

No.	$e^{l\,t}$	fSm/Nd	$^{143}Nd/^{144}Nd$ CHUR	$^{143}Nd/^{144}Nd$ initial	eNd actual	eNd initial
1	0.0082	-0.23	0.511023	0.511288	-2.1	5.2
2	0.0082	-0.47	0.511023	0.511681	-2.1	12.9
4	0.0082	-0.73	0.511023	0.511323	-17.2	5.9
5	0.0043	-0.53	0.511800	0.512391	2.8	11.5
7	0.0043	-0.53	0.511800	0.512354	2.1	10.8
8	0.0043	-0.41	0.511800	0.512274	2.6	9.3
9	0.0043	-0.51	0.511800	0.512314	1.7	10
10	0.0043	-0.56	0.511800	0.512377	2.1	11.3

The reactivation of old deep-seated faults during the Paleoproterozoic, the Permo-Triassic, the Cretaceous and the Cenozoic (Jelsma et al., 2009) probably is an important

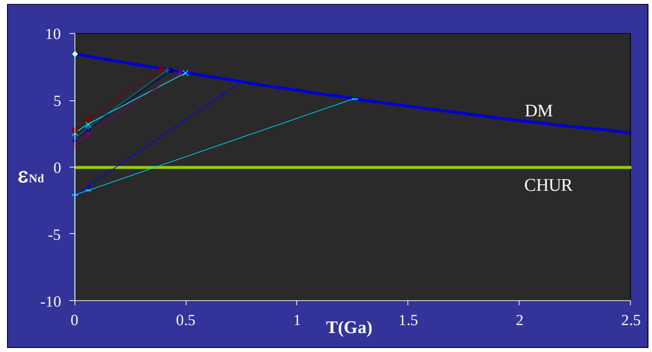

Fig. 2. Diagram of ε_{Nd} versus T (Ga) for xenoliths from the CA, CU79, and CU80 kimberlite pipes.

factor in some of the different pulses of diamondiferous kimberlites. Thus petrography, geochemistry and Sm-Nd isotopic data from these kimberlites becomes an interesting tool to recognize possible diamondiferous kimberlites in the area.

Acknowledgments

This research is funded by the CGL2005-07885/BTE and CGL2006-12973 projects of the Ministerio de Educación y Ciencia (Spain), and the AGAUR SGR 589 of the Generalitat de Catalunya. The first author (SRC) received a FI and a BE grant, both sponsored by the Departament d'Educació i Universitats de la Generalitat de Catalunya and the European Social Fund. We also thank ENDIAMA and the mine geologists from the CA and the CU79 pipes, especially Dr. M. Watangua and Dr. V. Pervov, who allowed us to acquire samples for this study and provided facilities for the mine trip. We also wish to thank Dr. A. Olimpio, Universidade Agostinho Neto, who helped with logistics and coordination. Thanks to the Serveis Cientificotècnics de la Universitat de Barcelona for assistance in the use of SEM/ESEM-BSE-EDS and EPMA analyses (E. Prats, R. Fontarnau†, Dr. J. García Veigas, and X. Llovet).

References

Egorov, K.N., Roman'ko, E.F., Podvysotsky, V.T., Sablukov, S.M., Garanin, V.K., D'yakonov, D.B., 2007. New data on kimberlite magmatism in southwestern Angola. Russian Geology and Geophysics 48 (4), 323-336, doi:10.1016/j.rgg.2006.08.001.

Jelsma, H., Barnett, W., Richards, S., Lister, G., 2009. Tectonic setting of kimberlites. Lithos 112 (S1), 55-165.

Perevalov, O.V, Voinovsky, A.S., Tselikovsky, A.F., Agueev, Y.L., Polskoi, F.R., Khódirev, V.L., Kondrátiev, A.I., 1992. Geología de Angola. Notícia explicativa da carta geológica á escala 1:1.000.000. Serviço Geológico de Angola. Lunda, pp. 135.

McDougall, J.D., Haggerty, S.E., 1999.. Ultradeep xenoliths from African kimberlites: Sr and Nd isotopic compositions suggest complex history. Earth and Planetary Science Letters 170, 73–82.

McLean, H., Banas, A., Creighton, S., Whiteford, S., Luth, R.W., Stachel, T., 2007. Garnet xenocrysts from the Diavik mine, NWT, Canada: Composition, color, and paragenesis. Canadian Mineralogist 45, 1131-1145.

Reis, B., 1972. Preliminary note on the distribution and tectonic control of kimberlites in Angola. Abstract 24th International Geological Congress, Rep. Sess. 4, 276-281, Montreal.

Weis, D, Kieffer, B., Maerschalk, C., Barling, J., de Jong, J., Williams, G.A., Hanano, D., Pretorius, W., Mattielli, N., Scoates, J.S., Goolaerts, A., Friedman, R.M., Mahoney, J.B., 2006. High-precision isotopic characterization of USGS reference materials by TIMS and MC-ICP-MS. Geochemistry, Geophysics, Geosystems 7, Q08006, doi:10.1029/2006GC001283.

Woodhead, J.D., Hergt, J.M., 2000. Pb-isotope analysis of USGS reference materials. Geostandards Newsletter 24 (1), 33–38.